International Journal of Wavelets, Multiresolution
and Information Processing
Vol. 3, No. 4 (2005) 587–599

World Scientific
www.worldscientific.com

A TIME ACCURATE PSEUDO-WAVELET SCHEME FOR TWO-DIMENSIONAL TURBULENCE

B. V. RATHISH KUMAR* and MANI MEHRA†

Department of Mathematics, Indian Institute of Technology
Kanpur, U.P., 208016, India
**bvrk@iitk.ac.in*
†*manimeh@iitk.ac.in*

In this paper, we propose a wavelet-Taylor–Galerkin method for solving the two-dimensional Navier–Stokes equations. The discretization in time is performed before the spatial discretization by introducing second-order generalization of the standard time stepping schemes with the help of Taylor series expansion in time step. Wavelet-Taylor–Galerkin schemes taking advantage of the wavelet bases capabilities to compress both functions and operators are presented. Results for two-dimensional turbulence are shown.

Keywords: Taylor–Galerkin method; wavelets; Navier–Stokes equations; turbulence.

AMS Subject Classification: 65M70, 76F99

1. Introduction

Turbulent flows are a grand challenge for numerical simulation. In such flows, there is a large range of active and important scales which all need to be resolved by a numerical mesh. It concerns practical purpose such as industrial or meteorological computations, as well as fundamental studies. Direct numerical simulation of turbulence requires the integration in time of the nonlinear Navier–Stokes equations. However, at a large Reynolds number, that is when nonlinear interactions are far dominant upon viscous effects, turbulent flows generate increasingly small scales. In consequence to be realistic, the discretization in space ought to handle a huge number of degrees of freedom. In dimension two, direct numerical simulation of homogeneous turbulent flows in the incompressible case can be performed up to quite large Reynolds numbers by way of spectral Fourier techniques. However, these Reynolds numbers are too low to compare to large scale atmospheric dynamics. The situation is much more difficult in dimension three where only moderate Reynolds are at hand even with the present largest supercomputers. In current approaches,

*Corresponding author.

the fine scales of the flow are replaced by a subgrid scale model, e.g., in Large Eddy Simulation (LES), using a linear cut-off filter which therefore does not depend on the actual flow realization.

Another property of turbulent flows is their strong intermittency. Turbulent flows are characterized by coherent structures, like vortex tubes or vortex sheets, which govern the dynamics and statistics of the flow. It is, therefore, quite intuitive to try to concentrate the numerical work on these structures since the coherent structures are spatially localized. From this property, one may dream on new basis functions more suitable to represent this intermittent spatial structure with only a few number of degrees of freedom. Wavelet methods have been associated, almost since their invention, to analyze the structure and dynamics of the flow.[1] These studies have shown that the strongest modes of the wavelet transform of a two-dimensional turbulent flow represent the coherent structure (e.g., vortices), the coherent vortices can be well represented by only a few wavelet modes. These observations suggest that wavelets could be an efficient basis for two-dimensional turbulent flows since the dynamics of such flows are largely controlled by their coherent vortices. From the mathematical properties of wavelet bases, where a field has a singularity of a given order, its wavelet coefficients at small scales grow at a related power of the scale.[2,3] This means that at a given scale, the number of degrees of freedom needed no longer depends on the scale itself but on the number of active singularities of the field at this scale. This property which comes from the double localization, in space and in scale, of the wavelets, has been used for analysis and compression of turbulent fields.[4] From a numerical point of the view, wavelets constitute optimal bases to represent functions with inhomogeneous regularity, such as intermittent turbulent flow fields.

In the conventional numerical approach to transient problems, the accuracy gained in using the high-order spatial discretization is partially lost due to the use of low-order time discretization schemes. Here, usually spatial discretization precedes the temporal discretization. On the contrary, the reversed order of discretization can lead to better time accurate schemes with improved stability properties. The fundamental idea behind the Taylor–Galerkin approach is the substitution of space derivatives for the time derivatives in Taylor series, as used in the derivation of the Lax–Wendroff method,[5] where in Taylor–Galerkin matrix resulting from wavelet Galerkin discretization, we are taking the advantage of wavelet compression because coherent structure is well represented by few non-zero wavelet modes.

The remainder of this paper is organized as follows. In the next section, we give a brief introduction to wavelets. In Sec. 3, we present the wavelet-Taylor–Galerkin method for advection-diffusion problem. In Sec. 4, the details of time-accurate pseudo-wavelet schemes for Navier–Stokes are given. In Sec. 5, we present the numerical results for linear advection-diffusion equation and for two-dimensional turbulence, the merger of two positive vortices pushed together by a weaker negative vortex. Conclusions are presented in Sec. 6.

2. Wavelet Preliminaries

In the following, we give a brief introduction to wavelets and our notation used. We first deal with one-dimensional wavelets and then consider two variants for its generalization to the multivariate case.

2.1. *Univariate wavelets*

A "Wavelet System" consists of the function $\phi(x)$ and the function $\psi(x)$ referred to as wavelet functions. We define translates of $\phi(x)$ as

$$\phi_i(x) = \phi(x - i). \tag{2.1}$$

Multiresolution analysis (MRA) is the theory that was used by Daubechies[6] to show that for any non-negative integer n, there exists an orthogonal wavelet with compact support such that all the derivatives up to order n exist. MRA describes a sequence of nested approximation spaces V_j in $L^2(R)$ such that closure of their union equals $L^2(R)$. MRA is characterized by the following axioms:

(i) $\overline{\{0\} \subset \cdots \subset V_{-1} \subset V_0 \subset V_1 \cdots \subset L^2(R)}$,
(ii) $\bigcup_{j=-\infty}^{j=\infty} V_j = L^2(R)$,
(iii) $\bigcap_{j \in Z} V_j = 0$,
(iv) $f \in V_j$ if and only if $f(2(\cdot)) \in V_{j+1}$,
(v) $\phi(x-k)_{k \in Z}$ is an orthonormal basis for V_0.

We define W_j to be the orthogonal complement of V_j in V_{j+1}, i.e. $V_j \perp W_j$ and

$$V_{j+1} = V_j + W_j. \tag{2.2}$$

$\phi_{j,k}(x) = 2^{j/2}\phi(2^j x - k)_{k \in Z}$ is an orthonormal basis for V_j and ϕ is the solution of so-called scaling equation

$$\phi(x) = \sqrt{2} \sum_{k=0}^{D-1} a_k \phi(2x - k) \tag{2.3}$$

with explicitly known coefficients a_k (lowpass filter). An analytical description of ϕ is not available, but it is also not needed. Wavelets are also dilates/translates of a single function ψ such that $\psi_{j,k} = 2^{j/2}\psi(2^j x - k)_{k \in Z}$ is an orthonormal basis for W_j. As pointed out by Meyer (1990), the complete toll box built in $L^2(R)$ can be used in the periodic case $L^2([0,1])$ by introducing a standard periodization technique. This technique consists at each scale in folding, around the integer values, the wavelet $\psi_{j,k}$ and the scaling functions $\phi_{j,k}$ centered in [0,1]. It writes $\tilde{\phi}_{j,l}(x) = \sum_{n=-\infty}^{\infty} \phi_{j,l}(x+n)$ and $\tilde{\psi}_{j,l}(x) = \sum_{n=-\infty}^{\infty} \psi_{j,l}(x+n)$ and generates V_{Pj} and W_{Pj}. A function $f \in V_{PJ}$ in pure periodic scaling function expansion $f(x) = \sum_{k=0}^{2^J-1} c_k^J \tilde{\phi}_{J,k}(x)$ and the periodic wavelet expansion $f(x) = \sum_{k=0}^{2^{J_0}-1} c_k^{J_0} \tilde{\phi}_{J_0,k}(x) + \sum_{j=J_0}^{J-1} \sum_{k=0}^{2^j-1} d_k^j \tilde{\psi}_{j,k}(x)$, where J_0 satisfy $0 \le J_0 \le J$ and the decay of the wavelet coefficient is given by the following theorem.[8]

Theorem 2.1. *Let $P = D/2$ be the number of vanishing moments for a wavelet $\psi_{j,k}$ and let $f \in C^P(R)$. Then, the wavelet coefficients decay as $|d_{j,k}| \leq C_P 2^{-j(P+\frac{1}{2})} \max_{\xi \in I_{j,k}} |f^{(P)}(\xi)|$.*

2.2. *Multivariate wavelets*

The simplest way to obtain multivariate wavelets is to employ anisotropic or isotropic tensor products.

(**MRA-d**) Here, the multivariate wavelets are defined by

$$\psi_{j,l}(x) := \psi_{(j_1,l_1)}(x_1) \dots \psi_{j_d,l_d}(x_d), \quad j := (j_1, \dots, j_d), \quad x, l \text{ analogous.}$$

(**MRA**) Here, anisotropy is avoided. The scaling functions are simply the tensor products of the univariate scaling functions. A two-dimensional MRA can be constructed from the following decomposition:

$$\begin{aligned} \boldsymbol{V}_j = V_j \otimes V_j &= (V_{j-1} \oplus W_{j-1}) \otimes (V_{j-1} \oplus W_{j-1}) \\ &= (W_{j-1} \otimes W_{j-1}) \oplus (W_{j-1} \otimes V_{j-1}) \oplus (V_{j-1} \\ &\quad \otimes W_{j-1}) \oplus V_{j-1} \otimes V_{j-1} \\ &= \boldsymbol{W}_{j-1} \oplus \boldsymbol{V}_{j-1}. \end{aligned}$$

Then, we have $\boldsymbol{V}_J = \boldsymbol{W}_{J-1} \oplus \cdots \oplus \boldsymbol{W}_0 \oplus \boldsymbol{V}_0$. The wavelet basis is given by

$$\{\psi_{j,k} \otimes \psi_{j,l}, \psi_{j,k} \otimes \phi_{j,l}, \phi_{j,k} \otimes \psi_{j,l}\}_{k,l \in Z, 0 \leq j \leq J-1} \cup \{\phi_{0,k} \otimes \phi_{0,l}\}_{k,l \in Z}.$$

We have used this MRA approach in our two-dimensional problem.

3. Wavelet-Taylor–Galerkin Method (W-TGM)

First to show our methodology, we are taking simple linear advection-diffusion equation $\partial_t u = -a\partial_x u + \nu \partial_x^2 u$ where a and $\nu > 0$ are positive constant coefficients.

We have used second-order W-TGM because too many terms are introduced in the third-order time derivative term, especially for nonlinear problems. This difficulty may be circumvented by the use of fractional-step approach[7] in which the advection-diffusion problem is decomposed into a pure advection problem followed by a pure diffusion problem. Where the advection phase may be treated by third-order W-TGM. Let us leave the spatial variable x continuous and discretize advection-diffusion equation in time by the following forward Taylor series expansion. To obtain an improved order of accuracy in δt we shall apply a Taylor–Galerkin method based on the following Taylor series expansions

$$u^{n+1} = u^n + \delta t u_t^n + \frac{\delta t^2}{2} u_{tt}^n + \cdots, \tag{3.1}$$

$$u^n = u^{n+1} - \delta t u_t^{n+1} + \frac{\delta t^2}{2} u_{tt}^{n+1} + \cdots. \tag{3.2}$$

Combination of these two gives

$$\frac{u^{n+1} - u^n}{\delta t} = \frac{1}{2}\left(u_t^n + u_t^{n+1}\right) + \frac{\delta t}{4}\left(u_{tt}^n - u_{tt}^{n+1}\right) \tag{3.3}$$

replacing the time derivatives by spatial derivatives, the associated wavelet-Taylor–Galerkin equations based on Crank Nicolsan (CN) time stepping scheme which includes first-order and second-order time derivatives. While the former is provided directly by governing PDE, the latter can be obtained by taking the time derivative of the governing PDEs. The time derivative is

$$u_{tt} = -a^2\partial_x^2 u - 2av\partial_x^3 u + v^2\partial_x^4 u \tag{3.4}$$

and the substitution of u_t and u_{tt} into the Taylor series expansion (3.3) gives W-TGM scheme

$$Au^{n+1} = Bu^n \tag{3.5}$$

where $A = I - \frac{\delta t}{2}\left(-a\partial_x u^n + \nu\partial_x^2\right) + \frac{\delta t^2}{4}\left(-a^2\partial_x^2 u - 2av\partial_x^3 u + v^2\partial_x^4 u\right)$ and $B = I + \frac{\delta t}{2}\left(-a\partial_x + \nu\partial_x^2\right) + \frac{\delta t^2}{4}\left(-a^2\partial_x^2 u - 2av\partial_x^3 u + v^2\partial_x^4 u\right)$. Now, wavelet-Galerkin discretization turns the problem into a finite-dimensional space.

$$d_u^{n+1} = \mathcal{A}^{-1}\mathcal{B}d_u^n = \mathcal{D}d_u^n. \tag{3.6}$$

In this finite-dimensional space, u^n is to be replaced by the vector d_u^n along a wavelet finite basis, and A and B are replaced by, respectively, $\mathcal{A}$ and $\mathcal{B}$ (finite) matrices. Due to second- and third-order terms in the Taylor series, our scheme leads to an implicit method that needs inversion. Now, to solve Eq. (3.6) in the wavelet basis, we will compute $\mathcal{A}^{-1}$ and $\mathcal{A}^{-1}\mathcal{B}$ once and store in compressed form. We can now give a computational procedure for computing (3.6) using wavelet compression.

Algorithm 1

(i) $trunc(\mathcal{A}^{-1}, \epsilon_M)$ --→ $(\mathcal{A}^{-1})^{\epsilon_M}$
(ii) compute initial guess in wavelet basis --→ d_u^0
(iii) $trunc(d_u^0, \epsilon_V)$ --→ $(d_u^0)^{\epsilon_V}$
(iv) for $n = 0, 1, \ldots, n1 - 1$
(v) $(\mathcal{A}^{-1})^{\epsilon_M}\mathcal{B}(d_u^n)^{\epsilon_V}$ --→ d_u^{n+1}
(vi) $trunc(d_u^{n+1}, \epsilon_V)$ --→ $(d_u^{n+1})^{\epsilon_V}$
(vii) endfor,

where $trunc(d_u, \epsilon_V) = \{d_k^j, |d_k^j| > \epsilon_V\}$ and $trunc(\mathcal{A}, \epsilon_M) = \{[A_{m,n}], [A_{m,n}] > \epsilon_M\}$.

A further property of the wavelet representation of operators is that the successive powers $\mathcal{D}^n$ of the time iteration matrix become sparser and sparser with increasing n. This property is very specific to wavelets, as the opposite occurs with finite difference where $\mathcal{D}^n$ becomes more and more dense a matrix as shown in Fig. 1. It is seen from Fig. 1 that in the wavelet-Taylor–Galerkin approach, compression in the matrix $\mathcal{D}^n$ is larger than the wavelet-Galerkin approach. From this property, we can obtain iterative speed of the wavelet-Taylor–Galerkin scheme.

Algorithm 2

(i) Initialize $(\mathcal{A}_0^{-1})^{\epsilon_M}$ and $(d_u^0)^{\epsilon_V}$
(ii) $(\mathcal{A}_0^{-1})^{\epsilon_M}\mathcal{B} \dashrightarrow (\mathcal{D}_0)^{\epsilon_M}$
(iii) for $n = 0, 1, \ldots, n1 - 1$
(iv) $(\mathcal{D}_n)^{\epsilon_M}(d_u^n)^{\epsilon_V} \dashrightarrow (d_u^{n+1})^{\epsilon_V}$
(v) $\mathcal{D}_n^2 \dashrightarrow \mathcal{D}_{n+1}$
(vi) endfor.

Then the approximate solution of PDE, at $t = 2^n\delta t$, is $d_u^{(2^n)}$.

Since differential operators are local operators, it seems that not much can be gained by compression. However, in wavelet basis it is possible to efficiently invert the differential operator and then approximate (in a compressed form) the dense evolution operators. There is no need to change from classical to wavelet coordinates until some time steps say p. In classical coordinates, the evolution operator changes from very sparse to dense. In the wavelet representation, we may start the squaring in the classical coordinates and change to the wavelet basis at the point where the wavelet representation is sparser. Thus, we have the following algorithm

Algorithm 3

(i) For $n = 0, 2, \ldots, p$
(ii) $(A)^{-1}Bu^n \dashrightarrow u^{n+1}$
(iii) Initialize $(\mathcal{A}^{-1})^{\epsilon_V}$ and $(d_u^p)^{\epsilon_V}$
(iv) for $n = p + 1, p + 2, \ldots, p + n1 - 1$
(v) $(\mathcal{A}^{-1})^{\epsilon_M}\mathcal{B}(d_u^n)^{\epsilon_V} \dashrightarrow (d_u^{n+1})$
(vi) $trunc(d_u^{n+1}, \epsilon_V) \dashrightarrow (d_u^{n+1})^{\epsilon_V}$.

It is essential for the success of this algorithm that the computation of the matrix vector product fully exploits the compressed form of both matrix and vectors. This can be done using the algorithm in Ref. 8 or fast multiplication based on a general sparse format for both matrix and vector.

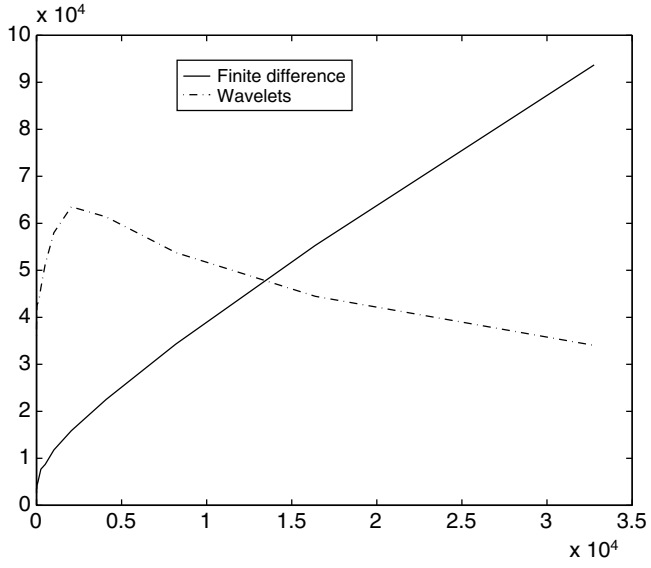

(a) CN times stepping in wavelets and in finite differences, versus $x = 2^n$, $n = 15$, $N = 1024$, $\nu\delta t = 10^{-5}$, $\epsilon_M = 10^{-8}$.

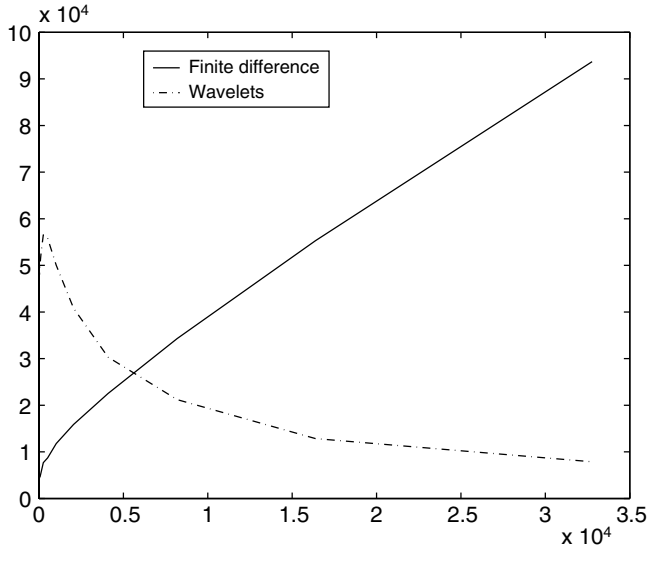

(b) Taylor–Galerkin approach in wavelets and in finite differences.

Fig. 1. Number of coefficients in the successive powers $\mathcal{D}^n$.

4. Wavelet-Taylor–Galerkin Schemes for Two-Dimensional Navier–Stokes Equations

4.1. *The Navier–Stokes equations*

A two-dimensional incompressible viscous flow is described by the Navier–Stokes equations. In vorticity/stream-function formulation:

$$-\Delta\psi = \omega,$$
$$\frac{\partial\omega}{\partial t} + J(\psi,\omega) = \nu\nabla\omega + \operatorname{curl} f,$$

where ω is the vorticity field (curl of the non-divergent velocity field), ψ the stream function, f a forcing term and $J(\psi,\omega) = \psi_y\omega_x - \psi_x\omega_y$ the two-dimensional Jacobian operator. We will consider the problem in a doubly periodic square domain.

Rewriting these equations as follows:

$$-\Delta\psi = \omega. \tag{4.1}$$
$$\frac{\partial\omega}{\partial t} = \nu\nabla\omega + s, \tag{4.2}$$

with $s = \operatorname{curl} f - J(\psi,\omega)$, we can, at each time step, split the problem into three subproblems: solve a Poisson equation to obtain stream function from the vorticity, evaluate the nonlinear term and integrate the heat equation.

The kinetic energy of the system is defined as

$$E(t) = \frac{1}{2}\int_\Omega \mathbf{v}^2(\mathbf{x},t)dx, \tag{4.3}$$

where $\mathbf{v} = (u,v)$ and $\mathbf{x} = (x,y)$, and analogously the enstrophy is

$$Z(t) = \frac{1}{2}\int_\Omega \omega^2(\mathbf{x},t)dx. \tag{4.4}$$

The dissipation of energy and enstrophy are related in the following way:

$$d_t E = -2\nu Z, \quad d_t Z = -2\nu P, \tag{4.5}$$

where

$$P(t) = \frac{1}{2}\int_\Omega |\nabla\omega|^2 dx \tag{4.6}$$

denotes the palinstrophy.

The energy spectrum

$$E(k) = \frac{1}{2}\sum_{k-1/2<|\mathbf{k}|\le k+1/2} |\hat{\mathbf{v}}(\mathbf{k})|^2, \quad k \in Z \tag{4.7}$$

and enstrophy spectrum

$$Z(k) = \frac{1}{2}\sum_{k-1/2<|\mathbf{k}|\le k+1/2} |\hat{\omega}(\mathbf{k})|^2, \quad k \in Z \tag{4.8}$$

are defined using the Fourier transform $\hat{f}(k) = \frac{1}{4\pi^2}\int_\Omega f(\mathbf{x})\exp(-i\mathbf{k}.\mathbf{x})dx$ with $\mathbf{k} = (k_x, k_y)$ and $|\mathbf{k}|^2 = k_x^2 + k_y^2$. The energy and enstrophy spectra are related according to the expression $Z(k) = |\mathbf{k}|^2 E(k)$.

4.2. *Wavelet-Taylor–Galerkin schemes for Navier–Stokes*

This scheme can be sketched as follows:
In the following, we will denote by $\tilde{\omega}$ the vorticity represented by its wavelet coefficient (the same notation holds for ψ and s. Starting from $\tilde{\omega}^n$ at time $t = n\delta t$:

(i) Compute $\tilde{\psi}^n$ by solving Poisson equation (4.2). Here, we can use the time iterative scheme algorithm 2 as described in Sec. 3, where the numerical solution has been searched as the long time asymptotic solution of the heat equation with the same forcing term on right-hand side.
(ii) Perform inverse wavelet transform to obtain nodal values ψ^n and ω^n.
(iii) Compute the nonlinear r.h.s s^n by collocation method using a second-order, energy enstrophy conserving, Arakawa's scheme.[9]
(iv) Compute the $\tilde{s}^n$ by s^n.
(v) Finally solve the heat equation (4.2) using the wavelet-Taylor–Galerkin schemes based on forward time stepping to obtain $\tilde{\omega}^{n+1}$, where the second-order time derivative is expressed in mixed form as $\omega_{tt} = \nu\omega_t + [(\nu\nabla\omega - J(\psi,\omega))_x\psi_y - \psi_x(\nu\nabla\omega - J(\psi,\omega))_y]$.

5. Numerical Results

5.1. *Case 1*

The accuracy of the proposed W-TGM has been verified numerically on the classical test problem of advection-diffusion of a Gaussian profile. The exact solution is $u(x,t) = (1/\sigma(t))\exp[-(x - x_0 - at)^2/2\sigma(t)^2]$, where $\sigma(t) = \sigma_0\big(1 + 2vt/\sigma_0^2\big)^{1/2}$. The parameters given by $h = 0.25, x_0 = 3.75, a = 1$. Figure 2 shows the comparison of numerical solution obtained for $\delta t = 10^{-3}$ using $D6$ scaling function with the exact solution. W-TGM scheme has been verified to be asymptotic stable.[10] The vector $u^{\epsilon_M,\epsilon_V}$ is the computed solution given the threshold ϵ_M and ϵ_V. Hence, we define the relative compression error as

$$E^{\epsilon_M,\epsilon_V} = \frac{\|u^{\epsilon_M,\epsilon_V} - u^{0,0}\|_\infty}{\|u^{0,0}\|_\infty}.$$

Table 1 shows the relative error introduced by compression $E^{\epsilon_M,\epsilon_V}$. It is seen from Fig. 1 that significant compression is achieved in matrix $\mathcal{D}^n$ and in the Taylor–Galerkin approach, the number of elements in matrix $\mathcal{D}^n$ is decaying faster than the wavelet-Galerkin approach. Hence, our W-TGM scheme can take much advantage of wavelet compression. Here, significant compression is also achieved in solution vector.

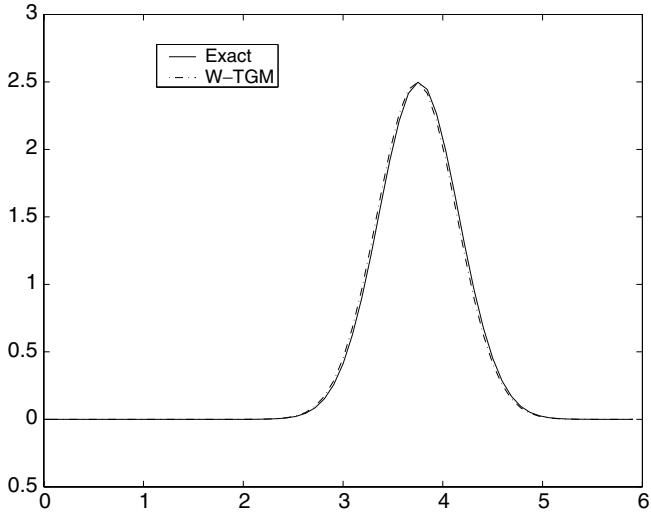

Fig. 2. Solution of advection-diffusion equation.

Table 1. Compression error for W-TGM scheme.

$\epsilon_V = 0$ ϵ_M	% elem $(\mathcal{A}^{-1})^{\epsilon_M}$	$E^{\epsilon_M,\epsilon_V}$	$\epsilon_M = 0$ ϵ_V	% elem $(d_u^n)^{\epsilon_V}$	$E^{\epsilon_M,\epsilon_V}$
10^{-10}	18.31	$8.6e-11$	10^{-10}	88.28	$6.6e-10$
10^{-9}	17.64	$6.2e-10$	10^{-9}	85.16	$2.4e-09$
10^{-8}	16.88	$4.6e-9$	10^{-8}	80.47	$3.3e-08$
10^{-7}	15.81	$1.3e-07$	10^{-7}	74.22	$3.3e-07$
10^{-6}	13.61	$2.4e-05$	10^{-6}	67.19	$4.7e-06$

5.2. *Case 2*

The numerical experiment we present studies the merging of two same sign vortices. It concerns free decaying turbulence (no forcing term). The initial condition for the simulation considered is

$$\omega(x,y) = \sum_{i=1}^{i=3} A_i \exp\big(-((x-x_i)^2 + (y-y_i)^2)/\sigma_i^2\big)$$

with variables $\sigma_i = 1/\pi$, amplitudes $A_1 = A_2 = -2A_3 = \pi$, and positions $x_1 = 3\pi/4, x_2 = x_3 = 5\pi/4$, $y_1 = y_2 = \pi, y_3 = \pi(1 + 1/(9\sigma_2))$. The initial conditions are quite specific, but the general dynamics of the vortex merger should not depend critically on the precise arrangement of the vortices. In fully developed two-dimensional turbulent flows, the chance of vortex merging increases with the density of vortices. Here, with only three vortices, we need this specific configuration to ensure a rapid merger; the negative vortex effectively replaces the mean field which pushes vortices together and induces merging. In fact, the configuration

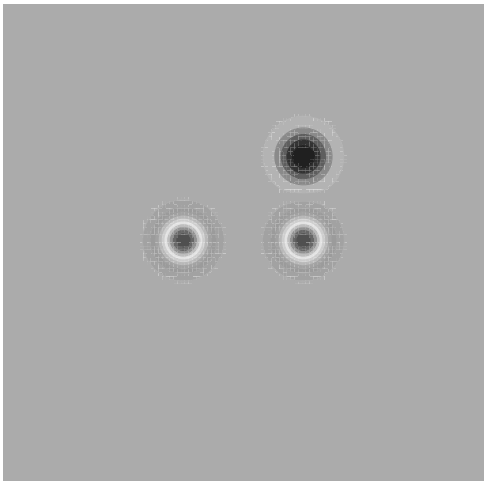

Fig. 3. Three vortex interaction: initial state ($t = 0$).

we have chosen should be fairly realistic since in practice, mergers are often caused by a fast-moving dipole running into another vortex: this is modeled by the three-vortex initial condition. The initial state is displayed in Fig. 3. In a $2\pi \times 2\pi$ box, three vortices with a Gaussian vorticity profile are present where two are positive with the same intensity (π) and the other one is negative with half the intensity of others.

The maximal scale J is 8 which corresponds to a maximum of $256 \times 256 = 65{,}536$ degrees of freedom. Further parameters are $\delta t = 2.5 \times 10^{-3}$, $\nu = 5 \times 10^{-5}$. The turnover time of one of the positive vortices is initially $T = 4.0$, and the initial Reynolds number based on the circulation of one of the positive vortices is $Re = 2 \times 10^4$. Note that since there is no external forcing, the energy and enstrophy decay monotonically in time. We determined that the thresholds used in the wavelet compression $\epsilon_v = 10^{-8}, \epsilon_M = 10^{-8}$ give satisfactory results. The vorticity fields at times $t = 10$, $t = 20$, $t = 30$ and $t = 40$ are displayed in Fig. 4. The comparison of energy spectra at times $t = 0$, $t = 20$, $t = 40$ are shown in Fig. 5.

6. Conclusion

We derived wavelet-based time accurate schemes for the two-dimensional incompressible Navier–Stokes equations. Our wavelet-based time accurate schemes take advantage of the compression of both the vorticity field and the operator involved, e.g., $(I - \delta t \nu \partial^2/\partial x^2)^{-1}$, in the wavelet bases in order to simulate two-dimensional turbulence with a reduced number of non-zero elements. The schemes have been successfully used in the computational simulation of merging of three vortices. The problem of vortex merging interaction is chosen because it has the strongest nonlinear interaction typical of two-dimensional turbulence.

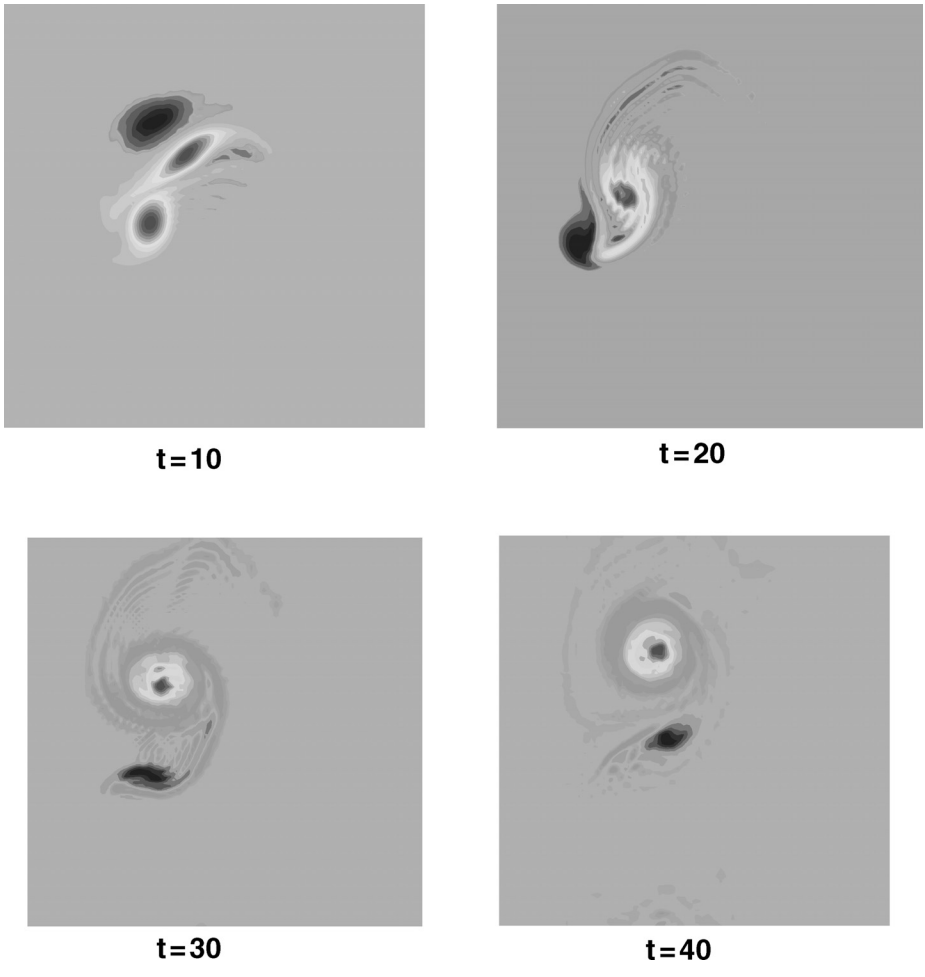

Fig. 4. Three-vortex interaction at different times.

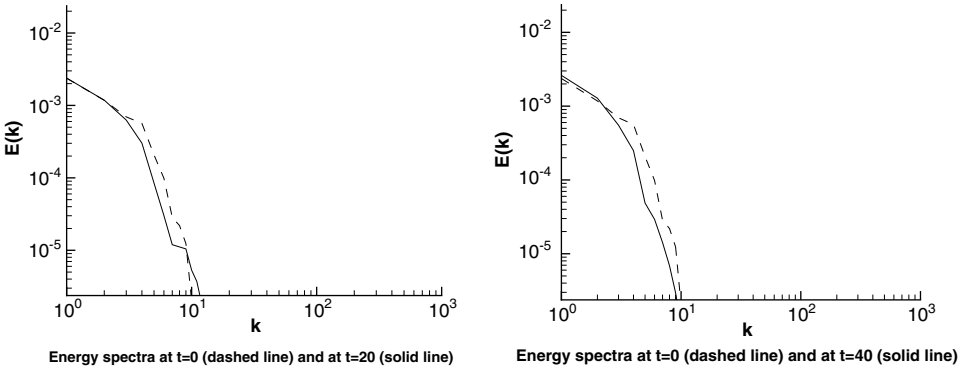

Fig. 5. Comparison of energy spectra.

References

1. M. Farge, J. F. Colonna and M. Holschneider, Wavelet analysis of coherent structure in two-dimensional turbulent flows, in *Topological Fluid Mechanics* (Cambridge University Press, 1990).
2. M. Holschneider and P. Tchamitchian, Pointwise regularity of Riemann's "nowhere differentiable" function, *Inventiones Mathematicae* **105** (1991) 157–175.
3. S. Jaffard and Y. Meyer, Wavelet methods for pointwise regularity and local oscillations of functions, *Mem. Amer. Math. Soc.* **123** (1996).
4. M. Farge, N. Kevlahan, V. Perrier and E. Goirand, Wavelets and turbulence, *Proc. IEEE* **84** (1996).
5. P. D. Lax and B. Wendroff, Systems of conservation laws, *Comm. Pure. Appl. Math.* **13** (1960) 217–237.
6. I. Daubechies, Orthonormal basis of compactly supported wavelets, *Comm. Pure Appl. Math.* **41** (1988) 906–966.
7. C. B. Jiang and M. Kawahara, The analysis of unsteady incompressible flows by a three-step finite element method, *Int. J. Numer. Meth. Fluids* **16** (1993) 793–811.
8. O. M. Nilsen, Wavelets in scientific computing, PhD thesis, Technical University of Denmark, Lyngby (1998).
9. A. Arakawa, Computational design for long-term numerical integration of the equations of the fluid motion: Two-dimensional incompressible flow. Part 1, *J. Comput. Phys.* **135** (1997) 103–114.
10. M. Mehra and B. V. Rathish Kumar, Time-accurate solution of advection-diffusion problems by wavelet-Taylor–Galerkin method, to appear in *Commun. Numer. Meth. Eng.*